AMERICAN SCIENTIFIC PUBLISHERS

Copyright © 2010 American Scientific Publishers
All rights reserved
Printed in the United States of America

Advanced Science Letters
Vol. 3, 379–384, 2010

Droplet Epitaxy of InN Quantum Dots on Si(111) by RF Plasma-Assisted Molecular Beam Epitaxy

Mahesh Kumar[1,2], Basanta Roul[1,2], Thirumaleshwara N. Bhat[1], Mohana K. Rajpalke[1], Neeraj Sinha[3], A. T. Kalghatgi[2], and S. B. Krupanidhi[1,*]

[1]*Materials Research Centre, Indian Institute of Science, Bangalore 560012, India*
[2]*Central Research Laboratory, Bharat Electronics, Bangalore 560013, India*
[3]*Office of Principal Scientific Advisor, Government of India, New Delhi 110011, India*

Delivered by Ingenta to:
Guest User
IP : 122.179.17.200
Mon, 01 Nov 2010 10:12:09

InN quantum dots (QDs) were fabricated on Si(111) substrate by droplet epitaxy using an RF plasma-assisted MBE system. Variation of the growth parameters, such as growth temperature and deposition time, allowed us to control the characteristic size and density of the QDs. As the growth temperature was increased from 100 °C to 300 °C, an enlargement of QD size and a drop in dot density were observed, which was led by the limitation of surface diffusion of adatoms with the limited thermal energy. Atomic force microscopy (AFM) and scanning electron microscopy (SEM) were used to assess the QDs size and density. The chemical bonding configurations of InN QDs were examined by X-ray photo-electron spectroscopy (XPS). Fourier transform infrared (FTIR) spectrum of the deposited InN QDs shows the presence of In–N bond. Temperature-dependent photoluminescence (PL) measurements showed that the emission peak energies of the InN QDs are sensitive to temperature and show a strong peak emission at 0.79 eV.

AMERICAN SCIENTIFIC PUBLISHERS

1. INTRODUCTION

Recently, semiconductor QDs have been studied extensively because of their unique physical properties and potential device applications. QDs of group-III nitride semiconductors have attracted because of their promising applications to optoelectronic and electronic devices, such as lasers, photo- detectors (PDs), light emitting diodes (LEDs) and high electron mobility transistors (HEMTs). InN is currently receiving much attention, in large part due to its recently observed narrow band gap E_g of 0.7–0.9 eV.[1–2] The direct band-gap transition in InN and its ability to form ternary (ex. InGaN) and quaternary (ex. AlInGaN) alloys increases the versatility of group-III nitride in optoelectronic devices in a broad spectrum ranging from near IR to UV. InN has the smallest effective electron mass of all the group-III nitrides, which leads to high mobility and high saturation velocity, and a large drift velocity at room temperature.[3–5] To fabricate III-nitride dots by self-assembly, the stranski–krastanow (SK) growth mode and recently, the droplet epitaxy (DE) technique has been utilized.[6–12] In DE technique, to convert the droplets into semiconductor nanocrystals, group III droplets are exposed to a subsequent group V molecular beam in DE-MBE approach. During this process, liquid metal droplet can be modified into various shapes of quantum structures and nanostructures.[3] Using DE technique, GaN quantum dots have been fabricated on Si(111) with RF-MBE.[14] Compared with other growth techniques, size and density control of the dots are easy in droplet epitaxy, because the density of the drops can be controlled by the amount of the supplied metals.

In this paper, we discuss the fabrication of InN QDs on Si(111) substrates using an RF plasma nitrogen source and the effects of growth temperature and growth time on size and density of the QDs.

2. EXPERIMENTAL DETAILS

All samples were grown in an RF- MBE system with a base pressure better than 1×10^{-10} mbar. The Si(111) substrates were ultrasonically degreased in isopropyl alcohol (IPA) for 10 min and boiled in trichloroethylene, acetone and methanol at 70 °C for 5 min, respectively, followed by dipping in 5% HF to remove the surface oxide. The substrates were outgassed at 900 °C for 1 h in ultra-high vacuum. After thermal cleaning, nitrogen plasma was switched on for 10 min at 540 °C substrate temperature, forming a nitridation layer on the surface, while keeping the plasma power and nitrogen flow rate at 350 W and 0.7 sccm, respectively,. The substrate was then exposed to an In molecular beam at different temperatures; 100 °C (sample (a)), 200 °C (sample (b)) and

*Author to whom correspondence should be addressed.

 1936-6612/2010/3/379/006 doi:10.1166/asl.2010.1163

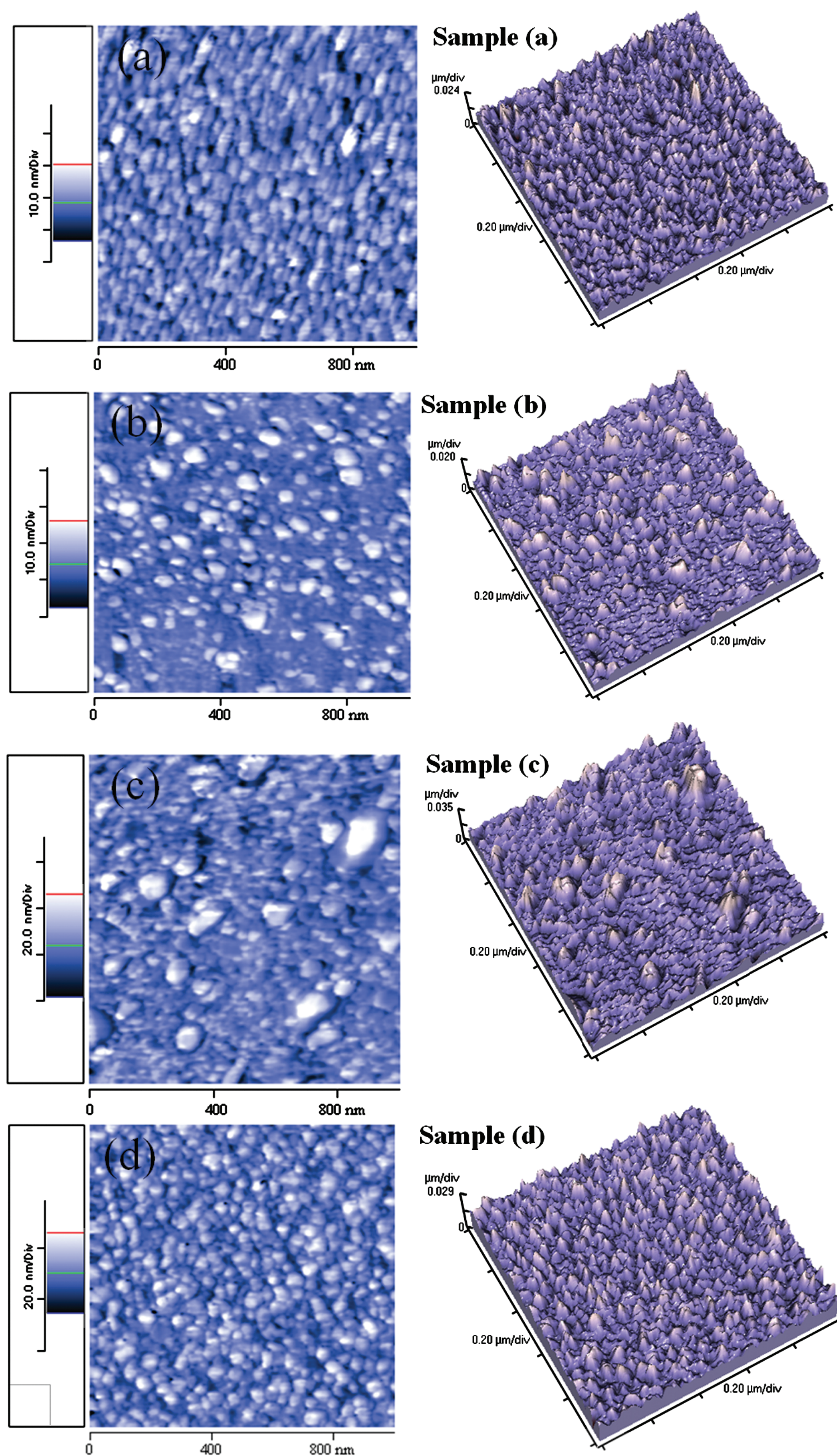

Fig. 1. AFM images of 1×1 μm^2 (2D and 3D) of InN QDs formed on Si(111) at different substrate temperatures (a) 100 °C (b) 200 °C (c) 300 °C for 120 sec In exposure time. Sample (b) was also subjected (d) for 180 sec.

Table I. Summary of average diameter and dot density under each set of growth conditions.

	(a)	(b)	(c)	(d)
Growth temp. (°C)	100	200	300	200
Growth time (sec.)	120	120	120	180
QDs diameter (nm)	25	51	64	52
QDs density (cm^{-2})	5.7×10^{10}	1.5×10^{10}	3.6×10^{9}	5.2×10^{10}

300 °C (sample (c)) to form In droplets and the exposed time was set to 120 seconds. For sample (d) the substrate temperature was kept at 200 °C and the exposed time was set to 180 seconds to vary the amount of In supplied. In cell temperature was kept at 830 °C and corresponding beam equivalent pressure (BEP) was 6.7×10^{-7} mbar. Next, the In droplets were exposed for 30 minutes with nitrogen plasma for nitridation of the In droplets. The nitrogen flow rate and plasma power were 0.7 sccm and 350 W, respectively. In addition, a post-growth annealing at 400 °C was carried out for all samples under nitrogen plasma for 30 minutes. The size and density of the grown InN QDs were investigated by AFM and SEM. The chemical bonding of the QDs on the surface were measured by XPS. The FTIR is used to monitor the chemical bonding structures of InN dots and the optical properties were investigated by PL measurements.

Delivered by Ingenta to:
Guest User
IP : 122.179.17.200
Mon, 01 Nov 2010 10:12:09

3. RESULTS AND DISCUSSION

The purpose of this study is to demonstrate the control over the size and density of InN QDs, which is demonstrated by two approaches. The first is by controlling the substrate temperature for fixed In exposure time and the second is by controlling exposure time of In at a fixed substrate temperature during the droplet formation. Figures 1(a–c) show the size and density control of InN droplets by controlling the substrate temperature for a fixed exposure time 120 seconds. Substrate temperature was varied from 100, 200 to 300 °C and average size of QDs are 25, 51 and 64 nm respectively as shown in Table I. The average size of droplets is increased with increasing substrate temperature but density of droplets is decreased. Figures 1(b and d) shows the size and density control of InN droplets with exposure time variation at a fixed substrate temperature. The In exposure time was varied from 120 to 180 sec. In this case the average size is almost same but density is drastically increased with exposure time.

The grown InN QDs were directly observed by *ex-situ* scanning electron microscopy. As illustrated in Figure 2, InN QDs are randomly distributed on the sample surface. The average QDs size is same as observed by AFM and density of droplets are 5.7×10^{10}, 1.5×10^{10}, 3.6×10^{9} and 5.2×10^{10} cm^{-2} for sample (a), (b), (c) and (d) respectively. The average size and density of droplets are plotted in Figure 3. The dimension of QDs is decreased with substrate temperature and this reduction in droplet dimensions can be ascribed to the limitation of surface diffusion of adatoms with the limited thermal energy. Overall, the average size of droplets is relatively larger and density is lower at higher substrate temperatures and vice versa. This is fairly an acceptable result as the surface diffusion of adatoms is lower at a lower surface temperature.[15–18]

The XPS was carried out to determine the composition of InN QDs using Al K_α radiation ($h\nu = 1486.6$ eV). Figure 4 shows the XPS spectra on untreated surface of sample (a) and also same peak values observed for other samples. Figure 4(a) shows a general scan in the binding energy ranging from 0 to 800 eV.

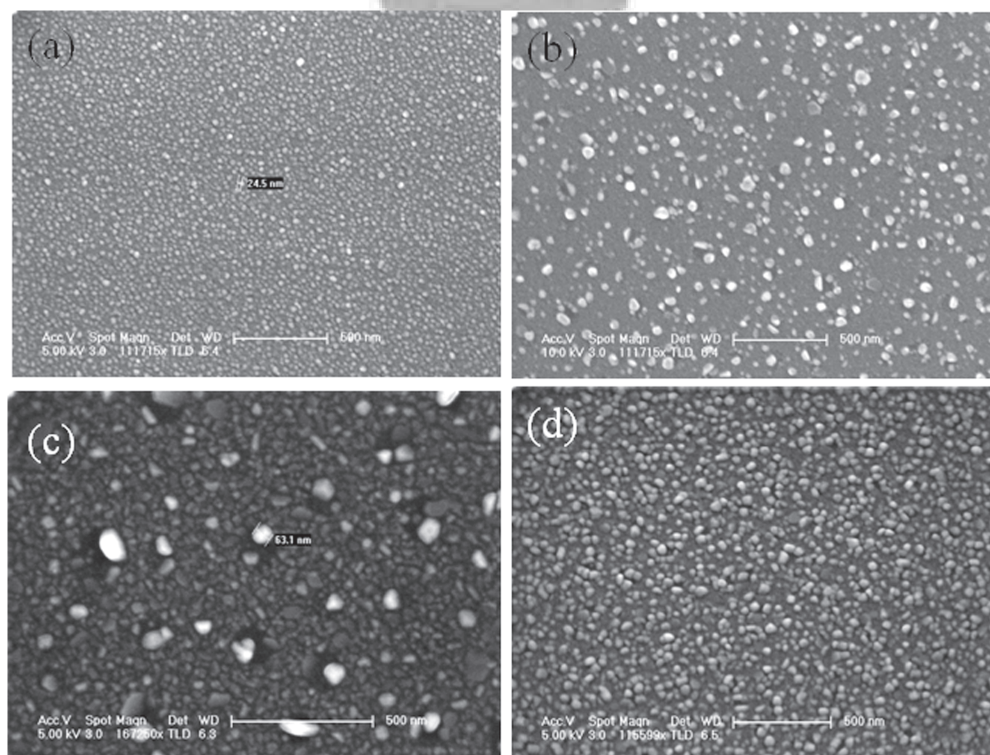

Fig. 2. SEM images of InN QDs formed on Si(111) at different substrate temperatures (a) 100 °C (b) 200 °C (c) 300 °C for 120 sec In exposure time. Sample (b) was also subjected (d) for 180 sec.

Adv. Sci. Lett. 3, 379–384, 2010

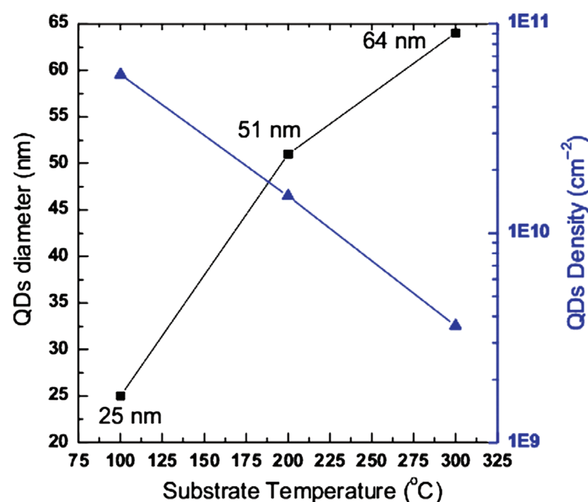

Fig. 3. Plot of size and density distribution of InN QDs by droplet epitaxy as a function of surface temperature. The density of droplets decreases as the substrate temperature increases but diameter show the opposite behavior.

The indium (In 4d, In 4p, In 4s, In $3d_{5/2}$, In $3d_{3/2}$, In $3p_{3/2}$, In $3p_{1/2}$), nitrogen (N 1s), carbon (C 1s) and oxygen (O 1s) peaks are observed. Figure 4(b) show the standard C 1s signal at 285.0 eV. Higher resolution spectra were taken of the In 3d region (Fig. 4(c)) and N 1s (Fig. 4(d)). The In core is spin–orbit split to the $3d_{5/2}$ peak at 444.2 eV and $3d_{3/2}$ peak at 451.7 eV. The peak at around 396.5 eV corresponds to N 1s of InN. These results are close to the reported values for bulk InN films.[19–20]

Figure 5 shows O 1s core-level spectra before and after cleaning. Before cleaning, the O 1s peak consists of a component at 532 eV due to adventitious oxygen (physisorbed rather than chemisorbed). According to Amanullah report,[21] generally the O 1s peak has been observed in the binding energy (BE) region of 529–535 eV. The peak at approximately 529–530 eV has been attributed to lattice oxygen. Ghuang et al.[22] have attributed the peak at approximately 530.7–531.6 eV to oxygen in non-stoichiometric oxides in the surface region. For chemisorbed O_2 on the metal surface, the BEs are found to be in the region 530–530.9 eV. Craciun et al.[23] have attributed the peak approximately at 532 eV to physisorbed oxygen on surface. Therefore, the O 1s peak observed for InN QDs before cleaning could be attributed to

Delivered by Ingenta to:
Guest User
IP : 122.179.17.200

Fig. 4. XPS spectra of InN QDs on untreated surface.

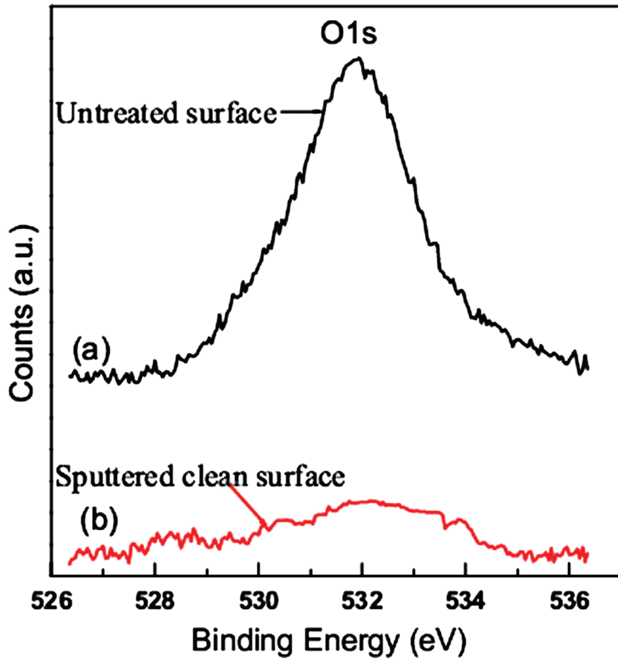

Fig. 5. O 1s core-level XPS spectra from (a) an untreated and (b) sputtered clean surface.

physisorbed oxygen. In Figure 4(b) C 1s spectra shows a shoulder component in the higher binding energy side, which also may be attributed to the physisorbed carbon monoxide.

The FTIR spectra of all samples were recorded in the range of 400 to 1400 cm^{-1}, while a representative spectrum is shown in Figure 6. The following infrared spectral bands were observed: 566.94, 611.30, 737.59, 819.51, 895.80 and 965.28 cm^{-1} and these values are in good agreement with reported band In–N

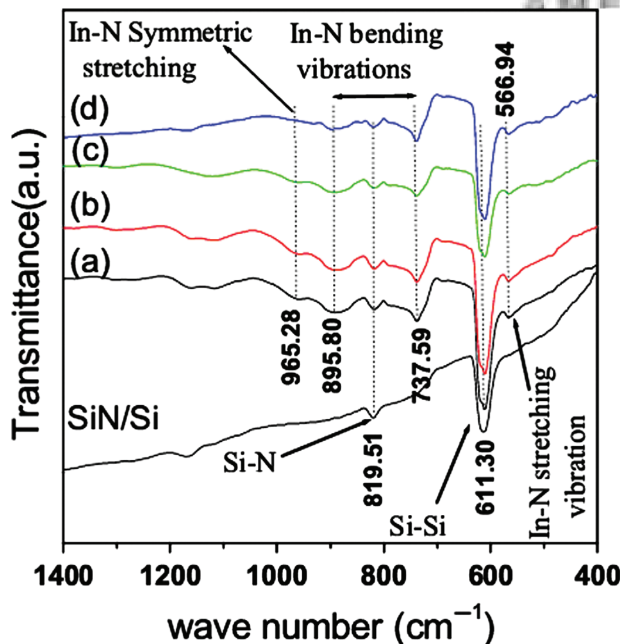

Fig. 6. FTIR Spectra of SiN on Si(111) (nitridation of Si(111)) and InN QDs on Si(111) substrate for sample (a), (b), (c) and (d).

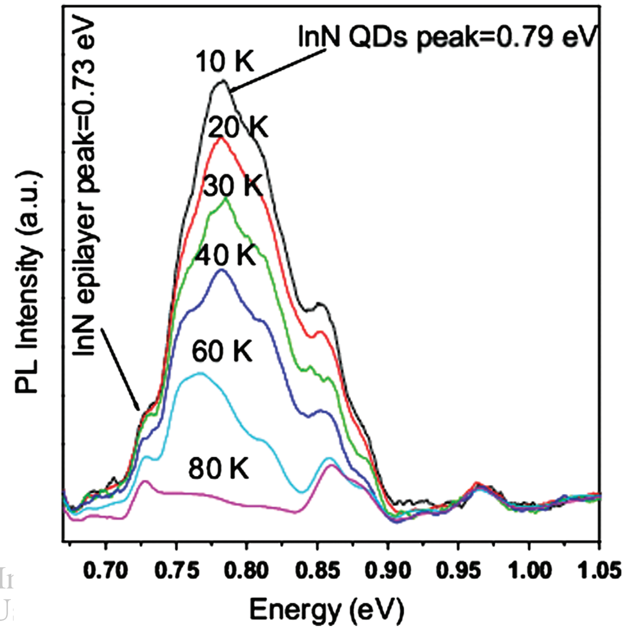

Fig. 7. Temperature-dependent PL Spectra of the InN QDs grown at 200 °C substrate temp and 180 sec In exposed time (sample (d)).

by Ir
est U
.179.17.200
Mon, 01 Nov 2010

stretching vibration at 570 cm^{-1},[24] bending vibrations at 735, 902 and symmetric stretching vibration at 968 cm^{-1} [25] in hexagonal InN films. The thickness of the silicon substrate is large compared to the InN QDs and hence a strong peak corresponding to Si–Si bond was observed at 611.30 cm^{-1}. From Figure 6 it can also be seen that the peak position at 819.51 cm^{-1} is corresponding to Si–N bond. No In–O peak is detected in IR spectra, which supports the XPS results of the formation of InN QDs.

Temperature-dependent PL spectra is shown in Figure 7 for the InN QDs grown at 200 °C substrate temp and 180 sec In exposed time (sample (d)) and it shows that the emission peak energies of the InN QDs are sensitive to temperature. In the PL spectra a strong peak at 0.79 eV and two weak peaks at 0.73 eV and 0.86 are observed. Notably, the PL spectrum contained multiple peaks and slightly blue shifted compared to the bulk InN, which may be due to the presence of InN QDs with different sizes in the sample and the size dependent quantum confinement effect, respectively. These emission energies are indicating, a thin layer of InN above the Si substrate followed by the InN QDs and a good agreement with reported band-gap energies.[26–27]

4. CONCLUSIONS

We have demonstrated the growth of InN QDs by droplet epitaxy technique on Si(111) substrate using RF-MBE. AFM and SEM measurements were performed to image the InN QDs directly and provided more detailed information on the dot size and density. It is illustrated that the dots size and density strongly depends on the growth temperature and deposition time. The XPS shows that the QDs synthesized are InN and it is also confirmed the O 1s peak observed before cleaning which is due to physisorbed oxygen. Spectral band values of InN QDs observed by FTIR are in good agreement with the reported InN films and the PL emission is highly efficient with a peak emission energy at 0.79 eV, which demonstrates the grown InN dots have good optical property.

References and Notes

1. J. Wu, W. Walukiewicz, K. M. Yu, J. W. Ager, III, E. E. Haller, H. Lu, W. J. Schaff, Y. Saito, and Y. Nanishi, *Appl. Phys. Lett.* 80, 3967 **(2002)**.
2. T. Matsuoka, H. Okamoto, M. Nakao, H. Harima, and E. Kurimoto, *Appl. Phys. Lett.* 81, 1246 **(2002)**.
3. S. N. Mohammad and H. Morkoc, *Prog. Quantum Electron.* 20, 361 **(1996)**.
4. E. Bellotti, B. F. Brennan, J. D. Albrecht, and L. F. Eastman, *J. Appl. Phys.* 85, 916 **(1999)**.
5. S. K. O'Leary, B. E. Foutz, M. S. Shur, U. V. Bhapkar, and L. F. Eastman, *J. Appl. Phys.* 83, 826 **(1997)**.
6. B. Daudin, F. Widmann, G. Feuillet, Y. Samson, M. Arlery, and J. L. Rouviere, *Phys. Rev. B* 56, R7069 **(1997)**.
7. C. Adelmann, N. Gogneau, E. Sarigiannidou, J. L. Rouviere, and B. Daudin, *Appl. Phys. Lett.* 81, 3064 **(2002)**.
8. N. Koguchi and K. Ishige, *Jpn. J. Appl. Phys.* 32, 2052 **(1993)**.
9. C. W. Hu, A. Bell, F. A. Ponce, D. J. Smith, and I. S. T. Tsong, *Appl. Phys. Lett.* 81, 3236 **(2002)**.
10. B. Chitara1, D. S. Ivan Jebakumar, C. N. R. Rao, and S. B. Krupanidhi, *Nanotechnology* 20, 405205 **(2009)**.
11. K. Kawasaki, D. Yamazaki, A. Kinoshita, H. Hirayama, K. Tsutsui, and Y. Aoyagi, *Appl. Phys. Lett.* 79, 2243 **(2001)**.
12. T. Maruyama, H. Otsubo, T. Kondo, Y. Yamamotob, and S. Naritsuka, *J. Cryst. Growth* 301/302, 486 **(2007)**.
13. J. H. Lee, Z. M. Wang, N. Y. Kim, and G. J. Salamo, *Nanotechnology* 20, 285602 **(2009)**.
14. C. L. Wu, L. J. Chou, and S. Gwo, *Appl. Phys. Lett.* 85, 2071 **(2004)**.
15. Y. Lee, E. Ahn, J. Kim, P. Moon, C. Yang, and E. Yoon, *Appl. Phys. Lett.* 90, 033105 **(2007)**.
16. E. A. Stinaff, M. Scheibner, A. S. Bracker, I. V. Ponomarev, V. L. Korenev, M. E. Ware, M. F. Doty, T. L. Reinecke, and D Gammon, *Science* 311, 636 **(2006)**.
17. Z. M. Wang, J. H. Lee, B. L. Liang, W. T. Black, P. K. Vas, Y. I. Mazur, and G. J. Salamo, *Appl. Phys. Lett.* 88, 233102 **(2006)**.
18. J. H. Lee, Z. M. Wang, Z. Y. Abuwaar, N. W. Strom, and G. J. Salamo, *Nanotechnology* 17, 3973 **(2006)**.
19. Y. Lu, L. Ma, and M. C. Lin, *J. Vac. Sci. Technol. A* 11, 2931 **(1993)**.
20. H. Parala, A. Devi, F. Hipler, E. Maile, A. Birkner, H. W. Becker, and R. A. Fischer, *J. Cryst. Growth* 231, 68 **(2001)**.
21. F. M. Amanullah, K. J. Pratap, and V. Hari Babu, *Mater. Sci. Eng. B* 52, 93 **(1998)**.
22. T. J. Ghuang, C. R. Brundle, and D. W. Rice. *Surf. Sci.* 59, 413 **(1979)**.
23. V. Craciun, J. M. Howard, D. Craciun, and R. K. Singh, *Appl. Surface Sci.* 2008–2009, 507 **(2003)**.
24. Y. C. Pan, W. H. Lee, C. K. Shu, H. C. Lin, C. I. Chiang, H. Chang, D. S. Lin, M. C. Lee, and W. K. Chen, *Jpn. J. Appl. Phys., Part 1* 38, 645 **(1999)**.
25. S. J. Patil, D. S. Bodas, A. B. Mandale, and S. A. Gangal, *Thin Solid Films* 52, 444 **(2003)**.
26. L. Brusaferri, S. Sanguinetti, E. Grilli, M. Guzzi, A. Bignazzi, F. Bogani, L. Carraresi, M. Colocci, A. Bosacchi, P. Frigeri, and S. Franchi, *Appl. Phys. Lett.* 69, 3354 **(1996)**.
27. M. C. Johnson, C. J. Lee, and E. D. Bourret-Courchesne, *Appl. Phys. Lett.* 85, 5670 **(2004)**.

Delivered by Ingenta to
Guest User
IP : 122.179.17.200
Mon, 01 Nov 2010 10:12:09

Received: 28 April 2010. Accepted: 28 May 2010.